

MOL #87775

**Glutamate-induced ATP synthesis: relationship between plasma membrane NCX and EAAT
in brain and heart cell models**

Simona Magi, Sara Arcangeli, Pasqualina Castaldo, Annamaria Assunta Nasti, Liberato Berrino,
Elena Piegari, Renato Bernardini, Salvatore Amoroso and Vincenzo Lariccia

*Department of Biomedical Sciences and Public Health, School of Medicine, University Politecnica
of Marche, Ancona, Italy (S.M., S.A., P.C., A.A.N., S.A., V.L.); Department of Experimental
Medicine, Second University of Naples, Naples, Italy (L.B., E.P.); Department of Clinical and
Molecular Biomedicine, School of Medicine, University of Catania, Catania, Italy (R.B.)*

MOL #87775

Running title: NCX plays a major role in Glu-induced energy metabolism

Corresponding author:

Salvatore Amoroso, MD

Department of Biomedical Sciences and Public Health

School of Medicine, University Politecnica of Marche

Via Tronto 10/A, 60126, Ancona, Italy

Tel. +39 071 2206176

Fax +39 071 2206178

Email: s.amoroso@univpm.it

Text pages-35

Tables-0

Figures-8

Supplemental Data: 1 figure

References-60

Words in Abstract-241

Words in Introduction-628

Words in Discussion-1500

List of abbreviations and chemical structures:

Bis-oxonol, bis (1,3-dibutylthiobarbituric acid)-trimethine oxonol; $[Ca^{2+}]_{cyt}$, intracytoplasmic Ca^{2+} concentration; DL-TBOA, DL-*threo*- β -Benzyloxyaspartic acid; EAAC1, Excitatory Amino Acid Carrier 1; EAATs, Excitatory Amino Acid Transporters; G418, Geneticin; GLAST, Glutamate–Aspartate Transporter; GLT1, Glutamate Transporter 1; Glu, Glutamate; KB-R7943, 2-[2-[4-phenyl]ethyl] isothiourea mesylate; NCX, Na^{+}/Ca^{2+} exchanger; $[Na^{+}]_i$, intracellular Na^{+}

MOL #87775

concentration; s.b.s., standard buffer solution; SN-6, 2-[[4-[(4Nitrophenyl) methoxy] phenyl] methyl]-4-thiazolidinecarboxylic acid ethyl ester; V_m , membrane potential; WT, Wild Type.

MOL #87775

Abstract

It is known that glutamate (Glu), the major excitatory amino acid in the central nervous system, can be an essential source for cell energy metabolism. Here we investigated the role of the plasma membrane $\text{Na}^+/\text{Ca}^{2+}$ exchanger (NCX) and the Excitatory Amino Acid Transporters (EAATs) in Glu uptake and recycling mechanisms leading to ATP synthesis. We used different cell lines, such as SH-SY5Y neuroblastoma, C6 glioma and H9c2 as neuronal, glial and cardiac models, respectively. We first observed that Glu increased ATP production in SH-SY5Y and C6 cells. Intriguingly, pharmacological inhibition of either EAAT or NCX counteracted the Glu-induced ATP synthesis. Furthermore, Glu induced a plasma membrane depolarization and an intracellular Ca^{2+} increase and both responses were again abolished by EAAT and NCX blockers. In line with the hypothesis of a mutual interplay between the activities of EAAT and NCX, coimmunoprecipitation studies showed a physical interaction between them. We expanded our studies on EAAT/NCX interplay in the H9c2 cells, used as cardiac model. H9c2 expresses EAATs but lacks of endogenous NCX1 expression. Interestingly, Glu failed to elicit any significant response in terms of ATP synthesis, cell depolarization and Ca^{2+} increase unless a functional NCX1 was introduced in H9c2 cells by stable transfection. Moreover, these responses were counteracted by EAAT and NCX blockers, as observed in SH-SY5Y and C6 cells. Collectively, these data suggest that plasma membrane EAAT and NCX are both involved in Glu-induced ATP synthesis, with NCX playing a pivotal role.

MOL #87775

Introduction

Glutamate (Glu), the major excitatory amino acid in the central nervous system of mammals, is involved in important brain functions such as memory and learning (Meldrum, 2000). Glu is also involved in brain energy metabolism, which is of fundamental importance to grant neuronal functions and survival (Hertz and Dienel, 2002). It has already been established that Glu per se is able to activate neuronal and glial energy metabolism (Hertz and Hertz, 2003; Magi et al., 2012; Panov et al., 2009). After being picked up by astrocytes/neurons, Glu can be converted to α -ketoglutarate that, as an intermediate of the Krebs cycle, can increase energy metabolism (Amaral et al., 2011; Olstad et al., 2007). The metabolic fate of Glu in the cells is influenced by its extracellular concentration as observed in astrocytes in which Glu is preferentially metabolized via Krebs cycle when its extracellular levels rise up to the low millimolar range (McKenna et al., 1996). Indeed, during synaptic stimulation, Glu can reach millimolar concentrations at the synaptic cleft (Clements et al., 1992; Danbolt, 2001; Nyitrai et al., 2006).

The extracellular concentration of Glu is spatially and temporally defined by a very efficient reuptake system located both in neuronal and glial cells, and composed of highly specialized proteins, the Excitatory Amino Acid Transporters (EAATs) (Danbolt, 2001). EAATs contribute to neurotransmitter recycling and prevent the extracellular Glu concentration from rising to neurotoxic levels (Maragakis and Rothstein, 2004). Recent studies indicate that EAATs may not be a mere glutamate “sink” that terminate glutamatergic synaptic transmission, but they can play a more important role in the control of cell energy metabolism than it was recognised before. In this regard, an association of Glutamate–Aspartate Transporter (GLAST) and Glutamate Transporter 1 (GLT-1), two members of EAATs family, with glycolytic enzymes and mitochondria has been reported (Bauer et al., 2012; Genda et al., 2011). Moreover, EAATs mitochondrial immunoreactivity was reported for three EAATs, namely GLAST (Magi et al., 2012; Ralphe et al., 2004), GLT-1 and Excitatory Amino Acid Carrier 1 (EAAC1) (Magi et al., 2012): the latter one is specifically

MOL #87775

involved in the Glu-dependent stimulation of ATP production in mitochondria isolated both from neuronal and glial cells (Magi et al., 2012).

Since EAATs transport Glu using the favorable Na^+ gradient (Tzingounis and Wadiche, 2007), a mechanism able to restore the transmembrane Na^+ gradient after Glu entry is required. Recent studies have suggested that the Na^+/K^+ -ATPase, the antiporter enzyme which maintains the Na^+ and K^+ ion gradients across the membrane, may regulate Glu uptake via EAATs (Bauer et al., 2012; Genda et al., 2011; Rose et al., 2009). However, a variable but significant component of the Na^+ -dependent Glu transport activity is resistant to ouabain at concentrations (0.1 – 5mM) known to inhibit the rat Na^+/K^+ -ATPase (Genda et al., 2011; Johansen et al., 1987; Rose et al., 2009; Volterra et al., 1994).

Another transporter that could support Glu entry via EAAT is the $\text{Na}^+/\text{Ca}^{2+}$ exchanger (NCX). NCX catalyzes the bidirectional and electrogenic exchange of 3 Na^+ and 1 Ca^{2+} across the plasma membrane, operating either in Ca^{2+} -efflux/ Na^+ -influx mode (*forward mode*) or Ca^{2+} -influx/ Na^+ -efflux mode (*reverse mode*) (Blaustein and Lederer, 1999; Torok, 2007). It has been already proposed that in astrocytes Glu and Na^+ entry via EAAT induces a Ca^{2+} response due to the reverse mode of plasma membrane NCX (Kirischuk et al., 2007; Verkhratsky, 2010). In a recent study we found that EAAT and NCX also localize within brain mitochondria and that EAAC1 and NCX1 exist as a macromolecular complex that allows Glu entry into the matrix, enhancing ATP production (Magi et al., 2012). In this paper we report findings suggesting that plasma membrane EAAT and NCX are involved in Glu-induced ATP synthesis in neuronal, glial and cardiac cells, and that NCX plays a pivotal role in this phenomenon.

MOL #87775

Materials and Methods

Cell Cultures

Cell lines (purchased from the American Type Culture Collection, Manassas, VA) were cultured as monolayer in polystyrene dishes (100 mm diameter) and grown in RPMI 1640 medium (SH-SY5Y cells) or DMEM medium (C6 and H9c2 cells) (Invitrogen, Carlsbad, CA) containing 10% heat-inactivated fetal bovine serum (Invitrogen), 1% L-glutamine (200 mM) (Invitrogen), 1% sodium pyruvate (100 mM) (Invitrogen), 100 IU/ml penicillin (Invitrogen), and 100 µg/ml streptomycin (Invitrogen). Cells were grown in a humidified incubator at 37°C in a 5% CO₂ atmosphere.

Generation and characterization of H9c2 cells stable expressing NCX1

H9c2 Wilde Type (WT) were plated at a density of 1.5×10^5 cells/cm², followed by culture in DMEM with 10% FBS. After 24 hours H9c2 cardiac myoblast were transfected with pcDNA3.1(+)-NCX1 (kindly provided by Dr K. D. Philipson) carrying the geneticin (G418) resistance gene, by using Lipofectamine reagent according to manufacture instructions. After additional 24 hours, cells were cultured with selection-medium containing G418 at the concentration of 500 µg/ml until control (untransfected) cells died completely. Individual foci from the transfected cells were then selected, subcultured, and transferred to other plates for further propagation. Clonal cells were cultured under the G418 selection-medium until a stable cell line (named H9c2-NCX1) was obtained, as revealed by Real Time-PCR, immunofluorescence analysis (data not shown) and western blot. For Real-Time the following primers were used: forward 5'-GCTCTGGTTCTGGAGGTTGATG-3' and reverse 5'-TTCTCCGGATGCTTCTGCTT-3'. NCX1 activity was evaluated in FLUO-4 loaded cells using a superfusion protocol designed to evoke Ca²⁺ uptake through the reverse mode. Briefly, H9c2-WT or H9c2-NCX1 cells were initially superfused with an extracellular solution containing (in mM) NaCl 140, KCl 5, HEPES 20, CaCl₂ 2, MgCl₂ 1,

MOL #87775

glucose 10. Then, NCX1 reverse mode was evoked by exposing the cells to a Na⁺-free solution containing (in mM) LiCl 140, KCl 5, HEPES 20, CaCl₂ 2, MgCl₂ 1, glucose 10. pH was adjusted to 7.1 in the Na⁺-based and Li⁺-based solutions with NaOH or LiOH, respectively. None of the H9c2-WT cells analyzed showed a Ca²⁺ response as observed in H9c2-NCX1 cells.

Antibodies

NCX1 protein was detected by using a commercially available mouse monoclonal IgG antibody (R3F1, Swant, Bellinzona, Switzerland, dilution 1:500). The following primary antibodies were used to detect EAATs: mouse anti-EAAC1 (Chemicon International, CA, USA, dilution 1:1000) (Castaldo et al., 2007; Levenson et al., 2002), rabbit anti-GLAST and rabbit anti-GLT1 (Castaldo et al., 2007) (both purchased from Alpha Diagnostic International and used at 1:1000 dilution).

Western blot and coimmunoprecipitation studies

Experiments were performed on whole lysates and plasma membrane crude fractions both from isolated brain tissue and continuous cell lines (i.e. SH-SY5Y human neuroblastoma, C6 rat glioma, H9c2 cardiac myoblast and H9c2 cells stably expressing NCX1). Whole lysates were obtained using standard techniques and a cell lysis solution containing (in mM): NaCl, 150; Tris-HCl (pH 7.4), 10; EDTA (pH 8.0), 1; SDS 1%, and a protease inhibitor cocktail mixture (Roche Diagnostics) while plasma membrane crude fractions were obtained as previously described (Castaldo et al., 2007). Briefly, cells and brain were homogenized in 6 vol. of ice-cold homogenizing buffer: 4 mM Tris-HCl, pH 7.4; 0.32 M sucrose, 1 mM EDTA; 0.25 mM dithiothreitol; protease inhibitor cocktail mixture tablets (Roche Diagnostics, Milan, Italy). Homogenates were centrifuged 1000×g at 4°C for 15 minutes, and supernatants were then centrifuged at 100,000×g at 4°C for 1 hour to obtain the crude membrane fraction. The pellet was resuspended in homogenizing buffer and stored at -70°C for immunoblotting.

MOL #87775

Cell membrane proteins were immunoprecipitated by using commercially available mouse monoclonal IgG antibodies directed against EAAC1 (1:50; Chemicon International) (Proper et al., 2002; Yu et al., 2006) and NCX1 (R3F1, 1:50; Swant) (Minelli et al., 2007). To recover the immunocomplexes, samples were incubated with A-Sepharose beads (GE Healthcare).

Proteins were separated by SDS-PAGE and transferred electrophoretically to a PVDF membrane and then incubated with the appropriate primary antibody. Immunoreactions were revealed by incubation with secondary antibody conjugated to horseradish peroxidase (Santa Cruz, CA, USA) (dilution 1:1000), for 1 hour at room temperature. An enhanced chemiluminescence detection system (ECLPlus; Amersham Biosciences) was used to detect bound antibodies. Images were captured and stored on a ChemiDoc station (BioRad, Milan, Italy), and analysed with the Quantity One (BioRad) analysis software (Castaldo et al., 2007).

Real-time confocal imaging

Measurement of membrane potential (V_m). SH-SY5Y, C6 and H9c2 cells grown for 18 hours on poly-L-lysine-coated glass coverslips were loaded for 1 hour at 37°C with the fluorescent anionic dye bis (1,3-dibutylthiobarbituric acid)-trimethine oxonol (bis-oxonol) 1 μ M (Molecular Probes, Eugene, OR), before each experiment (Ward et al., 2007). The dye is lipophilic and increases or decreases in fluorescence on depolarization or hyperpolarization, respectively. Importantly, the negative charge on bis-oxonol prevents accumulation in mitochondria; therefore, the dye distributes across cell membranes according to the V_m , giving a reliable measurement of relative changes in V_m (Mohr and Fewtrell, 1987). After bis-oxonol loading, cells were washed and transferred to a microscopy chamber in standard buffer solution (s.b.s.) in the presence of 1 μ M bis-oxonol. The dye was allowed to equilibrate for an average of 5 minutes, after which a stable baseline was obtained. Cells were then treated with the indicated compounds. Fluorescence was monitored with excitation at 530 nm and emission at 560-585 nm. Confocal images were obtained using the 510 LSM microscope equipped with a META detection system and a 20 \times objective. Illumination

MOL #87775

intensity was kept to a minimum (0.1–0.2% of laser output) to avoid phototoxicity; the pinhole was set to give an optical slice of $\sim 1\ \mu\text{m}$. For data analysis fluorescence was expressed as ratios (F/F_0) of fluorescence counts (F) relative to baseline values before stimulation (F_0). Data are presented as change in fluorescence relative to initial fluorescent value for each individual cell. Images were captured once every 30 seconds to avoid excessive bleaching of the dye. Cells on coverslips were then perfused with medium containing bis-oxonol ($1\ \mu\text{M}$) at constant rate and fluorescence imaging was started. When DL-threo-b-benzyloxyaspartic acid (DL-TBOA) ($300\ \mu\text{M}$), 2-[[4-[(4Nitrophenyl) methoxy] phenyl] methyl]-4-thiazolidinecarboxylic acid ethyl ester (SN-6) ($3\ \mu\text{M}$) or 2-[2-[4-phenyl]ethyl] isothiurea mesylate (KB-R7943) ($3\ \mu\text{M}$) were used, they were added starting from preincubation throughout the end of the experiments. Glu and/or added drugs were diluted in the perfusion medium and applied by switching the reservoirs of the perfusion system. Cell depolarization by perfusion with increased K^+ -containing extracellular solution was used as positive control (Supplemental Fig. 1). Na^+ in the high K^+ solution was reduced equivalently to maintain isosmolality.

Analysis of cytosolic Ca^{2+} ($\text{Ca}^{2+}_{\text{cyt}}$). Stock solutions of 5 mM Fluo-4 AM (Molecular Probes, USA) in DMSO (Molecular Probes, USA) were prepared and stored in aliquots at -20°C . SH-SY5Y, C6 and H9c2 cells were incubated with Fluo-4 AM (concentration $5\ \mu\text{M}$) for 50 minutes in the incubator at 37°C (Roychowdhury et al., 2006). Cells were superfused with standard buffer and were allowed to equilibrate for 15 minutes. For imaging of the Fluo-4 AM fluorescence, excitation light was provided by an argon laser at 488 nm and the emission was filtered with a 515 nm long pass filter. Images were acquired using the photomultiplier of the Zeiss LSM 510.

Analysis of fluorescence intensity was performed off-line after the image acquisition by averaging the fluorescence intensity values within boxes overlying the cell somata using the imaging software of Zeiss LSM. Data were normalized and the averages of the intensities were calculated.

MOL #87775

Analysis of ATP production

ATP production was evaluated by using a commercially available luciferase-luciferin system (ATPlite, Perkin Elmer). 24 hours after plating in 96 multiwell plates (60,000/well), cells were first washed with s. b. s. containing (in mM): NaCl, 140; KCl, 5; CaCl₂, 1; MgCl₂, 0.5; HEPES, 10; and glucose, 5.5, pH 7.4, adjusted with Tris, and then exposed to Glu (0.5–1 mM) in s. b. s. for 1 hour at 37°C. When ATP levels were evaluated in absence of extracellular Na⁺, NaCl was substituted with LiCl on an equimolar basis and pH was adjusted with LiOH. On the other hand, when experiments were conducted in Ca²⁺ free conditions, we substituted MgCl₂ for CaCl₂ in the extracellular solution. ATP levels were analyzed after incubation. All ATP data were normalized to the protein content.

Statistical analysis

Data were expressed as mean ± SEM. $p < 0.05$ was considered significant. Differences among means were assessed by one-way ANOVA followed by Dunnet's *post hoc* test.

Drugs and chemicals

DL-TBOA, DL-*threo*-β-Benzoyloxyaspartic acid; SN-6, 2-[[4-[(4Nitrophenyl) methoxy] phenyl] methyl]-4-thiazolidinecarboxylic acid ethyl ester and KB-R7943, 2-[2-[4-(4-Nitrobenzyloxy)phenyl]ethyl] isothiurea mesylate were obtained from Tocris. All the other chemicals were of analytical grade and were purchased from Sigma.

MOL #87775

Results

DL-TBOA inhibited Glu-induced ATP synthesis

As brain cell models, we initially used two cell lines, SH-SY5Y (neuroblastoma cell line) and C6 (glioma cell line) to test the effect of increasing concentrations of Glu, and we found a dose-dependent increase in ATP production with an EC₅₀ of 101.4 and 303 μ M respectively. These values are closely related to the K_m value for the Glu uptake estimated to be around 100 μ M (Danbolt, 2001). Interestingly, we found that the Glu-stimulated ATP synthesis in SH-SY5Y and C6 cell lines was counteracted by the non-transportable EAATs blocker DL-TBOA (Shigeri et al., 2004; Shimamoto et al., 1998) (Figs. 1A and B). Furthermore DL-TBOA per se had no effect on ATP levels (Figs. 1A and 1B).

Glu-induced plasma membrane depolarization

Considering that substrate uptake by EAATs is electrogenic (Danbolt, 2001; Kanai et al., 1993), the exposure of cells to increased Glu concentrations is expected to elicit a significant plasma membrane depolarization as a consequence of Na⁺ accumulation. This hypothesis was tested by real-time confocal videoimaging studies in cells loaded with the selective indicator of plasma membrane potential bis-oxonol (Parks et al., 2007). Exposure to Glu resulted in a significant depolarization both in SH-SY5Y and C6 cells (Figs. 2A-2D). In SH-SY5Y cells the increase in bis-oxonol fluorescence intensity was higher than that observed with high K⁺ evoked depolarization (Supplemental figure 1). At the present, we can speculate that this effect may depend on the cell type used. In line with previous results, in both cell lines, the depolarization was completely counteracted by DL-TBOA, confirming the key role of Na⁺/Glu co-transport in this response (Figs. 2A-2D).

MOL #87775

Involvement of NCX in Glu-induced ATP synthesis

Since plasma membrane EAATs co-transport Na^+/Glu , the maintenance of the Na^+ gradient is fundamental to their activities. We previously showed that in brain mitochondria Glu entry via EAAT requires a functional mitochondrial NCX (specifically NCX1) (Magi et al., 2012). Considering that NCX transporters are also expressed on cellular surface (Minelli et al., 2007; Torok, 2007), we tested the idea that an equivalent functional interaction between EAAT and NCX also exist for Glu entry into the cells. As shown in Figs. 2A-2D blockade of NCX conductance with KB-R7943 and SN-6 (Niu et al., 2007; Watanabe et al., 2006) completely prevented the Glu-induced depolarization in SH-SY5Y and C6 cells. In addition, we found that the two NCX inhibitors completely prevented Glu-induced ATP synthesis (Figs. 1C and 1D). Collectively these data suggest that NCX activity is critical for Glu-induced ATP synthesis. Membrane depolarization and intracellular Na^+ accumulation observed during Glu exposure may favour the reverse mode of operation of NCX which in turn will tend to bring Ca^{2+} into the cytoplasm (Rojas et al., 2013). Therefore, we measured $[\text{Ca}^{2+}]_{\text{cyt}}$ in SH-SY5Y and C6 cells before and after Glu exposure. Glu significantly increased $[\text{Ca}^{2+}]_{\text{cyt}}$ both in SH-SY5Y and C6 cells (Figs. 3A-3D). This effect was completely abolished by DL-TBOA and by the two NCX inhibitors, KB-R7943 and SN-6 (Figs. 3A-3D), confirming a close functional relationship between NCX and EAAT.

Finally, we found that all the pharmacological inhibitors (DL-TBOA, SN-6 and KB-R7943) had no effect on plasma membrane potential (Figs. 2E and 2F) and $[\text{Ca}^{2+}]_{\text{cyt}}$ (Figs. 3E and 3F).

Plasma membrane EAAT and NCX: physical interaction

We hypothesized that the functional interaction between NCX and EAAT could be consistent with their physical interaction. In a previous study (Magi et al., 2012) we demonstrated a physical link between NCX1 and EAAC1 within mitochondria, where the two transporters cooperate in the Glu-stimulated ATP synthesis. Since EAAC1 is the EAATs isoform predominately expressed in SH-SY5Y and C6 cells (Fig. 4A; (Magi et al., 2012)), we speculated that a similar relationship could

MOL #87775

exist on the plasma membrane. Coimmunoprecipitation studies performed on membrane protein fractions revealed a strong NCX1 immunoreactivity in the EAAC1 immunoprecipitates and, in line with this result, EAAC1 was pulled down by NCX1 antibody on reverse immunoprecipitation (Figs. 4B and 4C).

Plasma membrane EAAT and NCX functional interaction in cardiac cells

Glu is an important substrate for the intermediary metabolism not only in the brain but also in other organ such as the heart (Dinkelborg et al., 1996). Several studies have proposed that Glu plays an important role in the recovery of cardiac oxidative metabolism after ischemia (Kugler, 2004; Svedjeholm et al., 1996; Vanky et al., 2006). Similar to what observed in neuronal and glial cells, such metabolic response to extracellular Glu can only take place if cardiac cells express on their sarcolemma an efficient uptake system. Indeed, functional EAATs are expressed in cardiomyocytes (King et al., 2001; Kugler, 2004). We therefore hypothesized that also in heart the observed metabolic response elicited by Glu influx via EAAT could be regulated on cell surface by the cardiac isoform NCX1 (Menick et al., 2007; Shigekawa and Iwamoto, 2001). To test this possibility, we decided to use as cardiac model the rat heart derived H9c2 myoblasts (Menard et al., 1999). In preliminary experiments, we found that our H9c2 clone expresses three EAAT isoforms (GLAST, GLT1 and EAAC1) but lacks of endogenous expression of NCX1 (Fig. 5A), even after 7 days differentiation in 1% FBS or 10 nM retinoic acid (Menard et al., 1999) (data not shown). In addition, in this cell line we failed to detect any significant response to Glu stimulation in terms of ATP production, plasma membrane depolarization and $[Ca^{2+}]_{cyt}$ increase (Figs. 5B, 6A and 7A). We speculated that such unresponsiveness of H9c2 cells to Glu stimulation was due to the absence of NCX1. To confirm this, we decided to use our H9c2 cells (that we named H9c2-WT) and to generate an H9c2 clone (that we named H9c2-NCX1) by stable expressing a functional NCX1 (Fig. 5A, see Materials and Methods). NCX1 expression enabled H9c2 cells to respond to Glu, being ATP production stimulated, plasma membrane depolarization induced and $[Ca^{2+}]_{cyt}$ increased (Figs.

MOL #87775

5B, 6A and 7A). Concerning membrane depolarization in H9c2-NCX1, the increase in bis-oxonol fluorescence intensity was lower than that observed in SH-SY5Y and C6 cells and than that observed in the same cell line with high K^+ (Supplemental figure 1). We hypothesized that this effect may be related to specific cell type. Notably, both DL-TBOA and SN-6 counteracted all the Glu induced responses analyzed (Figs. 5C, 5D, 6C and 7C), but were without effects in unstimulated H9c2-NCX1 cells (Figs. 6B and 7B). Moreover, as observed in SH-SY5Y and C6 cells, coimmunoprecipitation studies performed on H9c2-NCX1 membrane protein extracts revealed a physical interaction between EAAC1 and NCX1 (Fig. 5A). In this regard, H9c2-WT cells, lacking endogenous NCX1 expression, provided a nice negative control to confirm the specificity of such interaction. Hence we carried out coimmunoprecipitation studies on this cell line. When membrane protein extracts from H9c2-WT were pulled down with NCX1 antibody, no immunoreactivity for EAAC1 was detected. Consistently with this result, no signal for NCX1 protein was detected when H9c2-WT protein membrane extracts were pulled down with EAAC1 (Fig. 5A).

Glu induced ATP synthesis: role of Ca^{2+} and Glu

Our results showed that exposure to Glu was able to increase ATP synthesis in both neuronal and non neuronal cells through the interplay between plasma membrane EAAT and NCX. We hypothesized a crucial role for NCX1, since by working on the reverse mode, it probably contribute to maintain the Na^+ gradient required for the EAAT activity. At the same time, as a consequence of NCX reverse mode activity, we observed an increase in $[Ca^{2+}]_{cyt.}$ that per se could represent a stimulus able to increase cellular ATP content through the activation of the mitochondrial Ca^{2+} dependent dehydrogenases (Denton, 2009). On the other hand, Glu per se is an important substrate that can be used by mitochondria to generate ATP. To definitely sort out these issues and clarify the mechanism underlying ATP production after Glu exposure, we tried to separately study the effect of Ca^{2+} and Glu.

MOL #87775

To evaluate the role of Ca^{2+} in absence of Glu, we measured the ATP content of C6, SH-SY5Y and H9c2-NCX1 cells after 1 hour exposure to a Na^+ free extracellular solution, known to evoke NCX reverse mode, and, consequently, to induce a rise in $[\text{Ca}^{2+}]_{\text{cyt}}$ ((Amoroso et al., 2000) and Fig. 5A). Conversely, to evaluate the role of Glu, we measured the ATP content of the same cell lines after 1 hour exposure to Glu in absence of extracellular Ca^{2+} . Interestingly, we observed that neither Ca^{2+} nor Glu were able to induce any significant increase in ATP content on their own. The increase in ATP synthesis occurred exclusively when cells were exposed to Glu in the presence of extracellular Ca^{2+} (Fig. 8).

MOL #87775

Discussion

The results of the present study showed that Glu (0.5-1mM) was able to increase ATP synthesis in SH-SY5Y (neuroblastoma) and C6 (glioma) cell lines used as model of neuronal and non neuronal cells, respectively. Both plasma membrane NCX and EAAT activities are required to elicit this metabolic response. This experimental evidence expanded our previous study in which we demonstrated a key role of the mitochondrial NCX and EAAT in Glu-induced ATP synthesis (Magi et al., 2012) and strengthened the earlier postulated role of Glu in brain energy metabolism (McKenna et al., 1996; Olstad et al., 2007). It is well known that as a neurotransmitter, the released Glu exerts its signalling function by interacting with specific receptors until it is removed from the extracellular fluid by the rapid uptake operated by EAATs (Danbolt, 2001; Kanai et al., 1993). The Glu taken up from the cells can be used as intermediary metabolite for ATP production (Hertz and Hertz, 2003; Panov et al., 2009) and, in this regard, a role for the EAATs-dependent uptake in brain cell energy metabolism has been also hypothesized (Bauer et al., 2012; Genda et al., 2011; Sonnewald et al., 1997), but at the moment scarce information are available on the role of EAATs in the metabolic response to Glu. Our results clearly showed that EAATs mediate Glu entry into the cells, leading to ATP production, since the non transportable EAATs inhibitor DL-TBOA (Anderson et al., 2001; Montiel et al., 2005; Shigeri et al., 2004; Shimamoto et al., 1998) completely prevented the metabolic response to Glu (Figs. 1A and 1B). EAATs are Na⁺-dependent transporters (Tzingounis and Wadiche, 2007) thus, consistently with the electrogenicity of EAATs Glu-uptake, a significant plasma membrane depolarization is expected to occur as a consequence of the Na⁺ entry. In line with this idea, we observed a Glu-induced and DL-TBOA-inhibited plasma membrane depolarization (Fig. 2). Because of the EAATs Na⁺ dependency, a mechanism is required in order to preserve the driving force provided by the transmembrane Na⁺ gradient after Glu entry. For this reason we tested the hypothesis that the plasma membrane NCX proteins could sustain EAATs activity by extruding the Na⁺ ions flowing into the cells with Glu. The blockade

MOL #87775

with specific inhibitors, such as KB-R7943 or SN-6 (Niu et al., 2007; Watanabe et al., 2006), completely prevented plasma membrane depolarization and Glu-mediated ATP increase both in SH-SY5Y and C6 cells (Figs. 1C, 1D and 2A, 2B, 2C, 2D), confirming that NCX, by operating on the reverse mode, can restore the Na^+ gradient and, consequently, sustain EAAT activity. If NCX is working on the reverse mode, then the Na^+ extrusion from the cytoplasm should be coupled to a Ca^{2+} entry and exposure to Glu is expected to elicit an increase in $[\text{Ca}^{2+}]_{\text{cyt}}$. Confocal videoimaging experiments with Fluo4-AM substantiated this hypothesis (Fig. 3), providing further evidence for a key role of NCX in the Glu-induced ATP synthesis. Notably, such Ca^{2+} response due to the reverse operation mode of NCX, was completely counteracted by KB-R7943 or SN-6 (Fig. 3). Obviously DL-TBOA was also able to block the $[\text{Ca}^{2+}]_{\text{cyt}}$ increase induced by Glu (Fig. 3). In this regard, Rojas and colleagues recently demonstrated that in rat cerebellar type-1 astrocytes the intracellular Ca^{2+} signal, induced by physiological concentration of the excitatory amino acid Glu and aspartate, is the result of the Na^+ entry through EAAT, that activates the reverse mode of NCX leading to Ca^{2+} entry (Rojas et al., 2013). It is also interesting to note that previous morphological observations showed that both EAAT (Danbolt, 2001) and NCX (Minelli et al., 2007) localized in the terminal processes of astroglial cells.

We have recently showed that EAATs are also expressed within mitochondria in various tissues (i.e. brain, heart) and cell lines (Magi et al., 2012). Such subcellular localization has a functional relevance, since these transporters contribute to the Glu-stimulated ATP synthesis (Magi et al., 2012). Notably, the mitochondrial EAAT-dependent Glu entry route is regulated by mitochondrial NCX (Magi et al., 2012). In particular, we reported that this mechanism relies on the selective interaction between a specific EAATs subtype - EAAC1 - and a specific NCX subtype - NCX1 -. Based on these findings, we tested the hypothesis that EAAC1 (the main EAATs isoform expressed by our cell lines (Magi et al., 2012) and NCX1 could also interact at plasma membrane level. We conducted coimmunoprecipitation studies both in SH-SY5Y and C6 cell isolated membrane

MOL #87775

fractions and, as showed in Fig. 4, we confirmed that NCX1 and EAAC1 associate even on cell surface as they do within mitochondria.

Collectively, these findings represent one of the main strengths of this paper, supporting the idea of a general mechanism where the cooperation between NCX1 and EAAC1 sustains brain energy metabolism, cooperation that can be relevant especially when ATP production is critically compromised such as in ischemia. In fact, during an ischemic insult cells massively release Glu, which in turn can lead to cell death immediately after the ischemia, but it might also be essential for the recovery of metabolic functionality in later stages (Ikonomidou and Turski, 2002). Effectively, Glu can participate in the recovery of energy production being used as intermediary metabolite for ATP synthesis, especially when the oxygen tension is not so low to abolish the oxidative metabolism, as it is observed in the ischemic penumbra and in the post-stroke recovery phases. The role of substrates alternative to glucose in supporting neuronal activity during and after hypoglycaemia has been recently explored *in vitro* and *in vivo* by using nuclear magnetic resonance (NMR), spectroscopy, and metabolic modelling (Amaral et al., 2011; Choi et al., 2001; Criego et al., 2005; Oz et al., 2009; Rao et al., 2010). In this regard, Sutherland and colleagues investigated how metabolism was processed in rat brain during and following recovery from profound hypoglycaemia (Sutherland et al., 2008). They provided evidence of a time-dependent increase in aspartate in parallel to a decrease in Glu/glutamine levels, and suggested that Glu, via aspartate aminotransferase, is the primary source of carbon when glucose-derived pyruvate is unavailable (Sutherland et al., 2008). A substantial net consumption of Glu during hypoglycaemia has also been documented by Rao and colleagues by monitoring the neurochemical profile in the hippocampus of 14 day old rats (Rao et al., 2010).

To further explore the physiological importance of the EAAC1-NCX1 relationship, we tested the possibility that a functional association between NCX1 and EAAC1 could be involved in the metabolic response to Glu not only in brain but also in the heart. Early evidence suggests that in cardiac tissue Glu exerts a protective action in ischemia by sustaining energy metabolism

MOL #87775

(Pisarenko et al., 1995). More recently, a putative protective role of Glu in myocardial infarction has been also postulated (Sivakumar et al., 2008; Sivakumar et al., 2011). However, to the best of our knowledge, no molecular mechanisms have been proposed. To this aim, we decided to use as cardiac model two cell clones, namely H9c2-WT (with no detectable endogenous NCX1 expression) and H9c2-NCX1 (constitutively expressing NCX1). Since both H9c2-WT and H9c2-NCX1 express GLAST, GLT-1 and EAAC1, these cell lines gave us the chance to specifically evaluate the importance of NCX1 in Glu-response. In line with the results obtained under NCX pharmacological blockade, in H9c2-WT Glu failed to induce any detectable response in terms of ATP synthesis, plasma membrane depolarization, and $[Ca^{2+}]_{cyt}$ increase (Figs. 5B, 6A and 7A). However, these DL-TBOA and SN-6 sensible responses were restored in H9c2-NCX1 cells (Figs. 5B, 5C and 5D; 6A, 6C and 7A, 7C), where we also detected the specific EAAC1-NCX1 physical interaction (Fig. 5A).

One may speculate that the increase in ATP content could be ascribed to the increase in $[Ca^{2+}]_{cyt}$ (Denton, 2009) occurring as a consequence of the hypothesized NCX reverse mode of operation. However, we observed that a rise in $[Ca^{2+}]_{cyt}$ was unable on its own to increase ATP levels in absence of Glu. Otherwise, Ca^{2+} plays a fundamental role, given that in absence of extracellular Ca^{2+} , Glu failed to induce any significant increase in ATP content (Fig. 8).

Therefore the following mechanism can be suggested: NCX activity maintains Na^+ gradient allowing Glu and Na^+ ions to enter into the cells. Moreover, the increase in $[Na^+]_i$ induces NCX-reverse mode, leading to $[Ca^{2+}]_{cyt}$ increase. Such increase can be buffered by mitochondria, stimulating Ca^{2+} -dependent dehydrogenases (Denton, 2009). This effect, in the presence of Glu as substrate, may contribute to the increase in ATP synthesis. Indeed, once in the cytoplasm, Glu can be taken up by mitochondria, where EAAC1 co-exist with NCX1 in a macromolecular complex as we previously described (Magi et al., 2012). Here NCX1 operates in the reverse mode to re-establish the Na^+ gradient across the mitochondrial membrane, further increasing mitochondrial

MOL #87775

Ca^{2+} concentration and Ca^{2+} -dependent dehydrogenases activity, with a concomitant increase in ATP synthesis.

In conclusion, we provide evidence that the EAAC1-NCX1 dependent influx pathway participates to the Glu-dependent metabolic response of neuronal and non-neuronal cells. The EAAC1-NCX1 interplay could have important implications, especially in pathological conditions. Future studies will try to address this hypothesis.

MOL #87775

Acknowledgements

The authors wish to thank Gerardo Galeazzi, Franco Pettinari and Carlo Alfredo Violet for their excellent technical assistance.

MOL #87775

Authorship Contributions

Participated in research design: Amoroso, Lariccia, Magi

Conducted experiments: Arcangeli, Castaldo, Lariccia, Magi, Nasti, Piegari

Performed data analysis: Amoroso, Bernardini, Berrino

*Wrote or contributed to the writing of the manuscript: Amoroso, Arcangeli, Bernardini, Berrino,
Lariccia, Magi*

MOL #87775

References

- Amaral AI, Teixeira AP, Sonnewald U and Alves PM (2011) Estimation of intracellular fluxes in cerebellar neurons after hypoglycemia: importance of the pyruvate recycling pathway and glutamine oxidation. *J Neurosci Res* **89**(5): 700-710.
- Amoroso S, Tortiglione A, Secondo A, Catalano A, Montagnani S, Di Renzo G and Annunziato L (2000) Sodium nitroprusside prevents chemical hypoxia-induced cell death through iron ions stimulating the activity of the Na⁺-Ca²⁺ exchanger in C6 glioma cells. *J Neurochem* **74**(4): 1505-1513.
- Anderson CM, Bridges RJ, Chamberlin AR, Shimamoto K, Yasuda-Kamatani Y and Swanson RA (2001) Differing effects of substrate and non-substrate transport inhibitors on glutamate uptake reversal. *J Neurochem* **79**(6): 1207-1216.
- Bauer DE, Jackson JG, Genda EN, Montoya MM, Yudkoff M and Robinson MB (2012) The glutamate transporter, GLAST, participates in a macromolecular complex that supports glutamate metabolism. *Neurochem Int* **61**(4): 566-574.
- Blaustein MP and Lederer WJ (1999) Sodium/calcium exchange: its physiological implications. *Physiol Rev* **79**(3): 763-854.
- Castaldo P, Magi S, Gaetani S, Cassano T, Ferraro L, Antonelli T, Amoroso S and Cuomo V (2007) Prenatal exposure to the cannabinoid receptor agonist WIN 55,212-2 increases glutamate uptake through overexpression of GLT1 and EAAC1 glutamate transporter subtypes in rat frontal cerebral cortex. *Neuropharmacology* **53**(3): 369-378.
- Choi IY, Lee SP, Kim SG and Gruetter R (2001) In vivo measurements of brain glucose transport using the reversible Michaelis-Menten model and simultaneous measurements of cerebral blood flow changes during hypoglycemia. *J Cereb Blood Flow Metab* **21**(6): 653-663.

MOL #87775

- Clements JD, Lester RA, Tong G, Jahr CE and Westbrook GL (1992) The time course of glutamate in the synaptic cleft. *Science* **258**(5087): 1498-1501.
- Criego AB, Tkac I, Kumar A, Thomas W, Gruetter R and Seaquist ER (2005) Brain glucose concentrations in patients with type 1 diabetes and hypoglycemia unawareness. *J Neurosci Res* **79**(1-2): 42-47.
- Danbolt NC (2001) Glutamate uptake. *Prog Neurobiol* **65**(1): 1-105.
- Denton RM (2009) Regulation of mitochondrial dehydrogenases by calcium ions. *Biochim Biophys Acta* **1787**(11): 1309-1316.
- Dinkelborg LM, Kinne RK and Grieshaber MK (1996) Transport and metabolism of L-glutamate during oxygenation, anoxia, and reoxygenation of rat cardiac myocytes. *Am J Physiol* **270**(5 Pt 2): H1825-1832.
- Genda EN, Jackson JG, Sheldon AL, Locke SF, Greco TM, O'Donnell JC, Spruce LA, Xiao R, Guo W, Putt M, Seeholzer S, Ischiropoulos H and Robinson MB (2011) Co-compartmentalization of the astroglial glutamate transporter, GLT-1, with glycolytic enzymes and mitochondria. *J Neurosci* **31**(50): 18275-18288.
- Hertz L and Dienel GA (2002) Energy metabolism in the brain. *Int Rev Neurobiol* **51**: 1-102.
- Hertz L and Hertz E (2003) Cataplerotic TCA cycle flux determined as glutamate-sustained oxygen consumption in primary cultures of astrocytes. *Neurochem Int* **43**(4-5): 355-361.
- Ikonomidou C and Turski L (2002) Why did NMDA receptor antagonists fail clinical trials for stroke and traumatic brain injury? *Lancet Neurol* **1**(6): 383-386.
- Johansen L, Roberg B and Kvamme E (1987) Uptake and release for glutamine and glutamate in a crude synaptosomal fraction from rat brain. *Neurochem Res* **12**(2): 135-140.
- Kanai Y, Smith CP and Hediger MA (1993) A new family of neurotransmitter transporters: the high-affinity glutamate transporters. *FASEB J* **7**(15): 1450-1459.

MOL #87775

- King N, Williams H, McGivan JD and Suleiman MS (2001) Characteristics of L-aspartate transport and expression of EAAC-1 in sarcolemmal vesicles and isolated cells from rat heart. *Cardiovasc Res* **52**(1): 84-94.
- Kirischuk S, Kettenmann H and Verkhratsky A (2007) Membrane currents and cytoplasmic sodium transients generated by glutamate transport in Bergmann glial cells. *Pflugers Arch* **454**(2): 245-252.
- Kugler P (2004) Expression of glutamate transporters in rat cardiomyocytes and their localization in the T-tubular system. *J Histochem Cytochem* **52**(10): 1385-1392.
- Levenson JM, Weeber EJ, Sweatt JD and Eskin A (2002) Glutamate uptake in synaptic plasticity: from mollusc to mammal. *Curr Mol Med* **2**(7): 593-603.
- Magi S, Lariccia V, Castaldo P, Arcangeli S, Nasti AA, Giordano A and Amoroso S (2012) Physical and functional interaction of NCX1 and EAAC1 transporters leading to glutamate-enhanced ATP production in brain mitochondria. *PLoS One* **7**(3): e34015.
- Maragakis NJ and Rothstein JD (2004) Glutamate transporters: animal models to neurologic disease. *Neurobiol Dis* **15**(3): 461-473.
- McKenna MC, Sonnewald U, Huang X, Stevenson J and Zielke HR (1996) Exogenous glutamate concentration regulates the metabolic fate of glutamate in astrocytes. *J Neurochem* **66**(1): 386-393.
- Meldrum BS (2000) Glutamate as a neurotransmitter in the brain: review of physiology and pathology. *J Nutr* **130**(4S Suppl): 1007S-1015S.
- Menard C, Pupier S, Mornet D, Kitzmann M, Nargeot J and Lory P (1999) Modulation of L-type calcium channel expression during retinoic acid-induced differentiation of H9C2 cardiac cells. *J Biol Chem* **274**(41): 29063-29070.
- Menick DR, Renaud L, Buchholz A, Muller JG, Zhou H, Kappler CS, Kubalak SW, Conway SJ and Xu L (2007) Regulation of Ncx1 gene expression in the normal and hypertrophic heart. *Ann N Y Acad Sci* **1099**: 195-203.

MOL #87775

- Minelli A, Castaldo P, Gobbi P, Salucci S, Magi S and Amoroso S (2007) Cellular and subcellular localization of Na⁺-Ca²⁺ exchanger protein isoforms, NCX1, NCX2, and NCX3 in cerebral cortex and hippocampus of adult rat. *Cell Calcium* **41**(3): 221-234.
- Mohr FC and Fewtrell C (1987) The relative contributions of extracellular and intracellular calcium to secretion from tumor mast cells. Multiple effects of the proton ionophore carbonyl cyanide m-chlorophenylhydrazone. *J Biol Chem* **262**(22): 10638-10643.
- Montiel T, Camacho A, Estrada-Sanchez AM and Massieu L (2005) Differential effects of the substrate inhibitor l-trans-pyrrolidine-2,4-dicarboxylate (PDC) and the non-substrate inhibitor DL-threo-beta-benzyloxyaspartate (DL-TBOA) of glutamate transporters on neuronal damage and extracellular amino acid levels in rat brain in vivo. *Neuroscience* **133**(3): 667-678.
- Niu CF, Watanabe Y, Ono K, Iwamoto T, Yamashita K, Satoh H, Urushida T, Hayashi H and Kimura J (2007) Characterization of SN-6, a novel Na⁺/Ca²⁺ exchange inhibitor in guinea pig cardiac ventricular myocytes. *Eur J Pharmacol* **573**(1-3): 161-169.
- Nyitrai G, Kekesi KA and Juhasz G (2006) Extracellular level of GABA and Glu: in vivo microdialysis-HPLC measurements. *Curr Top Med Chem* **6**(10): 935-940.
- Olstad E, Olsen GM, Qu H and Sonnewald U (2007) Pyruvate recycling in cultured neurons from cerebellum. *J Neurosci Res* **85**(15): 3318-3325.
- Oz G, Kumar A, Rao JP, Kodl CT, Chow L, Eberly LE and Seaquist ER (2009) Human brain glycogen metabolism during and after hypoglycemia. *Diabetes* **58**(9): 1978-1985.
- Panov A, Schonfeld P, Dikalov S, Hemendinger R, Bonkovsky HL and Brooks BR (2009) The neuromediator glutamate, through specific substrate interactions, enhances mitochondrial ATP production and reactive oxygen species generation in nonsynaptic brain mitochondria. *J Biol Chem* **284**(21): 14448-14456.

MOL #87775

- Parks SK, Tresguerres M and Goss GG (2007) Interactions between Na⁺ channels and Na⁺-HCO₃⁻ cotransporters in the freshwater fish gill MR cell: a model for transepithelial Na⁺ uptake. *Am J Physiol Cell Physiol* **292**(2): C935-944.
- Pisarenko OI, Studneva IM, Shulzhenko VS, Korchazhkina OV and Kapelko VI (1995) Substrate accessibility to cytosolic aspartate aminotransferase improves posthypoxic recovery of isolated rat heart. *Biochem Mol Med* **55**(2): 138-148.
- Proper EA, Hoogland G, Kappen SM, Jansen GH, Rensen MG, Schrama LH, van Veelen CW, van Rijen PC, van Nieuwenhuizen O, Gispen WH and de Graan PN (2002) Distribution of glutamate transporters in the hippocampus of patients with pharmaco-resistant temporal lobe epilepsy. *Brain* **125**(Pt 1): 32-43.
- Ralphe JC, Segar JL, Schutte BC and Scholz TD (2004) Localization and function of the brain excitatory amino acid transporter type 1 in cardiac mitochondria. *J Mol Cell Cardiol* **37**(1): 33-41.
- Rao R, Ennis K, Long JD, Ugurbil K, Gruetter R and Tkac I (2010) Neurochemical changes in the developing rat hippocampus during prolonged hypoglycemia. *J Neurochem* **114**(3): 728-738.
- Rojas H, Colina C, Ramos M, Benaïm G, Jaffe E, Caputo C and Di Polo R (2013) Sodium-Calcium Exchanger Modulates the L-Glutamate Ca(i) (2+) Signalling in Type-1 Cerebellar Astrocytes. *Adv Exp Med Biol* **961**: 267-274.
- Rose EM, Koo JC, Antflick JE, Ahmed SM, Angers S and Hampson DR (2009) Glutamate transporter coupling to Na,K-ATPase. *J Neurosci* **29**(25): 8143-8155.
- Roychowdhury S, Noack J, Engelmann M, Wolf G and Horn TF (2006) AMPA receptor-induced intracellular calcium response in the paraventricular nucleus is modulated by nitric oxide: calcium imaging in a hypothalamic organotypic cell culture model. *Nitric Oxide* **14**(4): 290-299.

MOL #87775

- Shigekawa M and Iwamoto T (2001) Cardiac Na⁽⁺⁾-Ca⁽²⁺⁾ exchange: molecular and pharmacological aspects. *Circ Res* **88**(9): 864-876.
- Shigeri Y, Seal RP and Shimamoto K (2004) Molecular pharmacology of glutamate transporters, EAATs and VGLUTs. *Brain Res Brain Res Rev* **45**(3): 250-265.
- Shimamoto K, Lebrun B, Yasuda-Kamatani Y, Sakaitani M, Shigeri Y, Yumoto N and Nakajima T (1998) DL-threo-beta-benzyloxyaspartate, a potent blocker of excitatory amino acid transporters. *Mol Pharmacol* **53**(2): 195-201.
- Sivakumar R, Anandh Babu PV and Shyamaladevi CS (2008) Protective effect of aspartate and glutamate on cardiac mitochondrial function during myocardial infarction in experimental rats. *Chem Biol Interact* **176**(2-3): 227-233.
- Sivakumar R, Babu PV and Shyamaladevi CS (2011) Aspartate and glutamate prevents isoproterenol-induced cardiac toxicity by alleviating oxidative stress in rats. *Exp Toxicol Pathol* **63**(1-2): 137-142.
- Sonnewald U, Westergaard N and Schousboe A (1997) Glutamate transport and metabolism in astrocytes. *Glia* **21**(1): 56-63.
- Sutherland GR, Tyson RL and Auer RN (2008) Truncation of the krebs cycle during hypoglycemic coma. *Med Chem* **4**(4): 379-385.
- Svedjeholm R, Vanhanen I, Hakanson E, Joachimsson PO, Jorfeldt L and Nilsson L (1996) Metabolic and hemodynamic effects of intravenous glutamate infusion early after coronary operations. *J Thorac Cardiovasc Surg* **112**(6): 1468-1477.
- Torok TL (2007) Electrogenic Na⁺/Ca²⁺-exchange of nerve and muscle cells. *Prog Neurobiol* **82**(6): 287-347.
- Tzingounis AV and Wadiche JI (2007) Glutamate transporters: confining runaway excitation by shaping synaptic transmission. *Nat Rev Neurosci* **8**(12): 935-947.

MOL #87775

- Vanky FB, Hakanson E, Jorfeldt L and Svedjeholm R (2006) Does glutamate influence myocardial and peripheral tissue metabolism after aortic valve replacement for aortic stenosis? *Clin Nutr* **25**(6): 913-922.
- Verkhatsky A (2010) Physiology of neuronal-glial networking. *Neurochem Int* **57**(4): 332-343.
- Volterra A, Trotti D, Tromba C, Floridi S and Racagni G (1994) Glutamate uptake inhibition by oxygen free radicals in rat cortical astrocytes. *J Neurosci* **14**(5 Pt 1): 2924-2932.
- Ward MW, Huber HJ, Weisova P, Dussmann H, Nicholls DG and Prehn JH (2007) Mitochondrial and plasma membrane potential of cultured cerebellar neurons during glutamate-induced necrosis, apoptosis, and tolerance. *J Neurosci* **27**(31): 8238-8249.
- Watanabe Y, Koide Y and Kimura J (2006) Topics on the Na⁺/Ca²⁺ exchanger: pharmacological characterization of Na⁺/Ca²⁺ exchanger inhibitors. *J Pharmacol Sci* **102**(1): 7-16.
- Yu YX, Shen L, Xia P, Tang YW, Bao L and Pei G (2006) Syntaxin 1A promotes the endocytic sorting of EAAC1 leading to inhibition of glutamate transport. *J Cell Sci* **119**(Pt 18): 3776-3787.

MOL #87775

Footnotes

This work was supported by “Ricerca Scientifica di Ateneo” and by “Regione Campania”.

MOL #87775

Figure Legends

Figure 1. Involvement of NCX and EAAT in Glu-stimulated ATP synthesis in SH-SY5Y and C6 cells.

ATP production in SH-SY5Y (A) and C6 (B) cells after 1 hour incubation with Glu (black bars) or vehicle (gray bars). DL-TBOA was able to counteract Glu-stimulated ATP synthesis in both cell lines. (C, D) KB-R7943 and SN-6 effect on Glu-induced ATP synthesis in SH-SY5Y and C6 cells, respectively. Both NCX inhibitors were able to counteract Glu-induced ATP synthesis. Cells were pre-incubated for 15 minutes with the inhibitors and then exposed to Glu (black bars) or vehicle (gray bars) for 1 hour. The drugs did not affect the energy level at the steady state. Each bar in panels A-D represents the mean of almost six different experiments.

* $p < 0.01$ vs any other group (Fig. 1A); * $p < 0.001$ vs any other group (Figs. 1B-D).

Figure 2. Real-time membrane potential analysis in intact cells (SH-SY5Y and C6).

Experiments performed in SH-SY5Y (A,C,E) and C6 (B,D,F) cells using the plasma membrane potential indicator bis-oxonol (1 μM). Glu perfusion induced plasma membrane depolarization (blue line). DL-TBOA (300 μM) (pink line), SN-6 (3 μM) (green line) and KB-R7943 (yellow line) (3 μM) all perfused from 20 minutes before through the end of recordings, prevented Glu-stimulated plasma membrane depolarization. For each group, more than 50 cells recorded in three different experimental sessions were analyzed and the maximal depolarization induced after Glu stimulation was used for the statistical analysis. * $p < 0.001$ vs any other group.

(E,F) Inhibitors did not have any significant effect on plasma membrane potential. For each group, more than 30 cells recorded in three different experimental sessions were analyzed.

MOL #87775

Figure 3. Real-time intracellular Ca^{2+} analysis in intact cells (SH-SY5Y and C6).

Experiments performed in SH-SY5Y (A,C,E) and C6 (B,D,F) cells using the intracellular Ca^{2+} indicator Fluo-4 AM (5 μM). Glu perfusion induced an increase in intracellular Ca^{2+} levels (blue line). DL-TBOA (300 μM) (pink line), SN-6 (3 μM) (green line) and KB-R7943 (3 μM) (yellow line) all perfused from 20 minutes before through the end of recordings, prevented Glu-stimulated $[\text{Ca}^{2+}]_{\text{cyt}}$ increase. For each group, more than 50 cells recorded in three different experimental sessions were analyzed and the maximal $[\text{Ca}^{2+}]_{\text{cyt}}$ induced after Glu stimulation was used for the statistical analysis. * $p < 0.001$ vs any other group.

(E,F) Inhibitors did not have any significant effect on $[\text{Ca}^{2+}]_{\text{cyt}}$. For each group, more than 30 cells recorded in three different experimental sessions were analyzed.

Figure 4. NCX1-EAAC1 coimmunoprecipitation.

(A) Characterization of the EAAT isoforms expression by immunoblots on membrane protein fractions obtained from SH-SY5Y and C6 cells. Only EAAC1 protein expression was detected in both cell lines. (B,C) Coimmunoprecipitation experiments showing NCX1-EAAC1 physical interaction in SH-SY5Y and C6 cells. Membrane protein fractions (m) enriched with anti-NCX1 antibody (B) or EAAC1 antibody (C) by selective immunoprecipitation (Ip) were loaded onto the gel and the reactivity versus EAAC1 and NCX1, respectively, was evaluated. In each Ip lane, the lower bands represent the immunoglobulins.

Figure 5. Characterization of H9c2 cells and involvement of NCX and EAAT in Glu-stimulated ATP synthesis.

(A) Characterization of H9c2 cardiac myoblast. Immunoblot analysis showed NCX1 expression in H9c2-NCX1 transfected cells but not in the H9c2-WT. H9c2 cells showed positive immunoreactivity for GLT1, GLAST and EAAC1. On the bottom of panel A (right side), coimmunoprecipitation experiments performed in H9c2-NCX1 and H9c2-WT are showed. NCX1-

MOL #87775

EAAC1 physical interaction was detected in H9c2-NCX1, while in H9c2-WT membrane protein fractions coimmunoprecipitation experiments showed negative results, confirming the specificity of such interaction. Membrane protein fractions (m) and selective immunoprecipitation enriched with EAAC1 antibody or anti-NCX1 antibody (Ip) were loaded onto the gel and the reactivity versus NCX1 and EAAC1, respectively, was evaluated. In each Ip lane, the lower bands represent the immunoglobulins.

On the bottom of panel A (left side) the functional characterization of H9c2-NCX1 cells is showed: a representative trace (of average 60 cells) of Na^+ -free induced an increase in $[\text{Ca}^{2+}]_{\text{cyt}}$ in H9c2-NCX1 cells (red line). This phenomenon did not occur in H9c2-WT (black line). Each value is reported as % of its basal fluorescence. (B) In H9c2-WT cells (white bars) glutamate was not able to evoke ATP synthesis, while in H9c2-NCX1 cells (gray bars) Glu induced a remarkable increase in ATP production that was counteracted by DL-TBOA (C).

(D) Pharmacological inhibition exerted by SN-6 on glutamate-induced ATP synthesis in H9c2-NCX1 cells. Cells were pre-incubated for 15 minutes with the inhibitors and then exposed to glutamate (black bars) or vehicle (grey bars) for 1 hour. The drugs did not affect the energy level at the steady state. Each bar in panels B-D represents the mean of almost five different experiments. * $p < 0.05$ vs any other group (Fig. 5C); * $p < 0.001$ vs any other group (Figs. 5B and 5D).

Figure 6. Real-time membrane potential analysis in intact cells (H9c2).

(A) Experiments performed in H9c2-WT and H9c2-NCX1 cells using the plasma membrane potential indicator bis-oxonol (1 μM). Only H9c2-NCX1 (gray line) showed a significant plasma membrane depolarization. (B) Inhibitors did not have any significant effect on plasma membrane potential. For each group, more than 30 cells recorded in three different experimental sessions were analyzed. (C) In H9c2-NCX1 cells DL-TBOA (300 μM) (blue lines) and SN-6 (3 μM) (pink lines), all perfused from 20 minutes before through the end of recordings, prevented Glu-stimulated plasma membrane depolarization. For each group, more than 50 cells recorded in three different

MOL #87775

experimental sessions were analyzed and the maximal depolarization induced after glutamate stimulation was used for the statistical analysis. * $p < 0.001$ vs any other group.

Figure 7. Real time intracellular Ca^{2+} analysis in intact cells (H9c2).

(A) Experiments performed in H9c2-WT and H9c2-NCX1 cells using the intracellular Ca^{2+} indicator Fluo-4 AM (5 μM). Only H9c2-NCX1 (gray line) showed a remarkable increase in $[\text{Ca}^{2+}]_{\text{cyt}}$. (B) Inhibitors did not have any significant effect on $[\text{Ca}^{2+}]_{\text{cyt}}$. For each group, more than 30 cells recorded in three different experimental sessions were analyzed. (C) In H9c2-NCX1 cells DL-TBOA (300 μM) (blue lines) and SN-6 (3 μM) (pink lines), all perfused from 20 minutes before through the end of recordings, prevented Glu-stimulated increase in $[\text{Ca}^{2+}]_{\text{cyt}}$. For each group, more than 50 cells recorded in three different sessions were analyzed and the maximal depolarization induced after glutamate stimulation was used for the statistical analysis. * $p < 0.001$ vs any other group.

Figure 8. Effect of Ca^{2+} and Glu on ATP synthesis.

ATP production in SH-SY5Y (A), C6 (B) and H9c2-NCX1 (C) after 1 hour exposure to Glu both in presence and absence of extracellular Ca^{2+} . ATP production was also evaluated in absence of Glu in a Na^+ -free extracellular solution able to evoke an increase in $[\text{Ca}^{2+}]_{\text{cyt}}$. For all the three cell lines analyzed, the increase in ATP synthesis occurred exclusively when cells were exposed to Glu in the presence of extracellular Ca^{2+} .

Each bar represents the mean of six different experiment for SH-SY5Y cells and of ten different experiments for C6 and H9c2-NCX1 cells.

* $p < 0.001$ vs any other group (Figs. 8A and 8B); * $p < 0.001$ vs Ctrl s.b.s., Ctrl 0Ca^{2+} , Ctrl $0\text{Ca}^{2+} + \text{Glu}$; # $p < 0.05$ vs 0Na^+ (Fig. 8C).

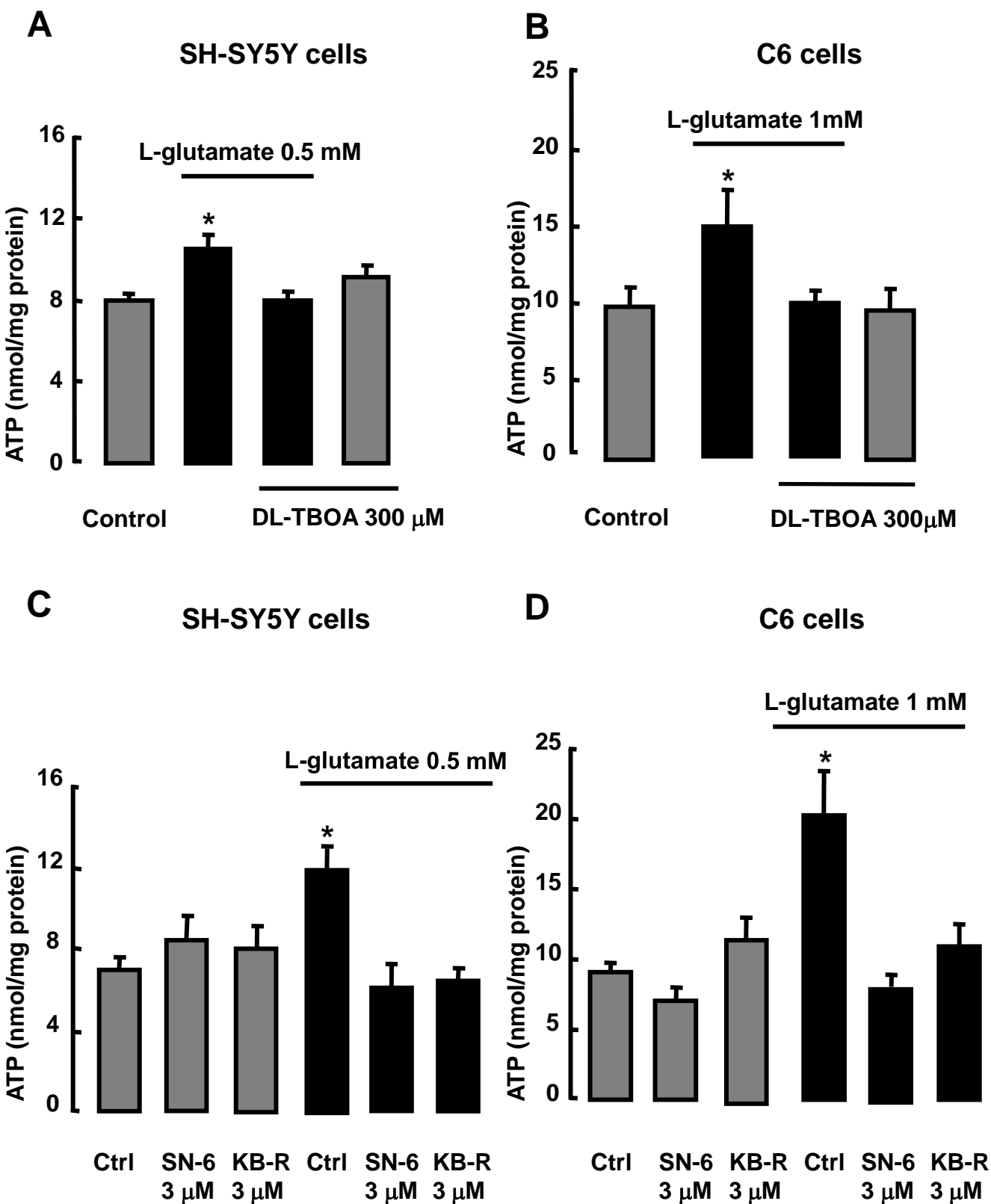


Figure 1

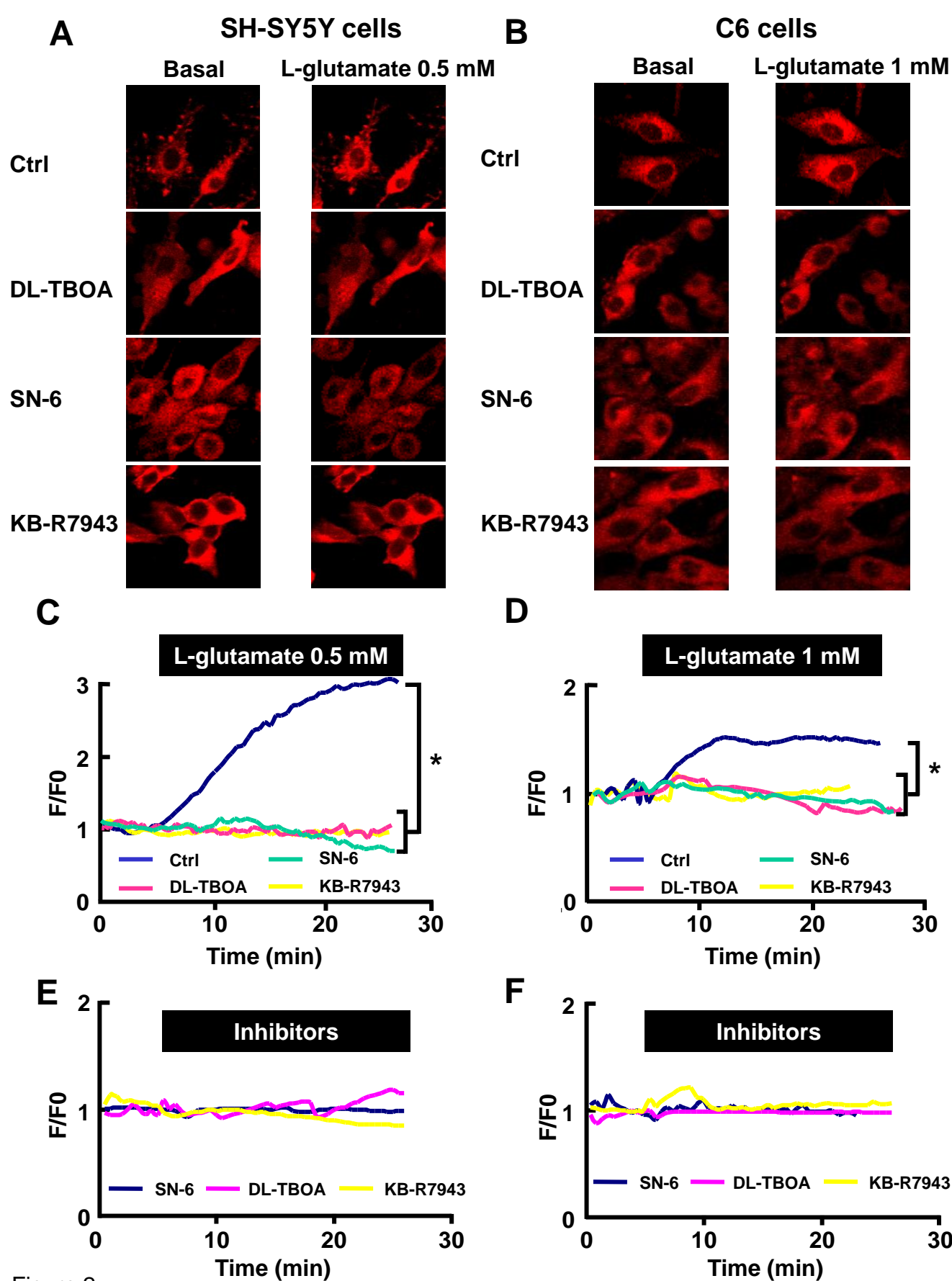


Figure 2

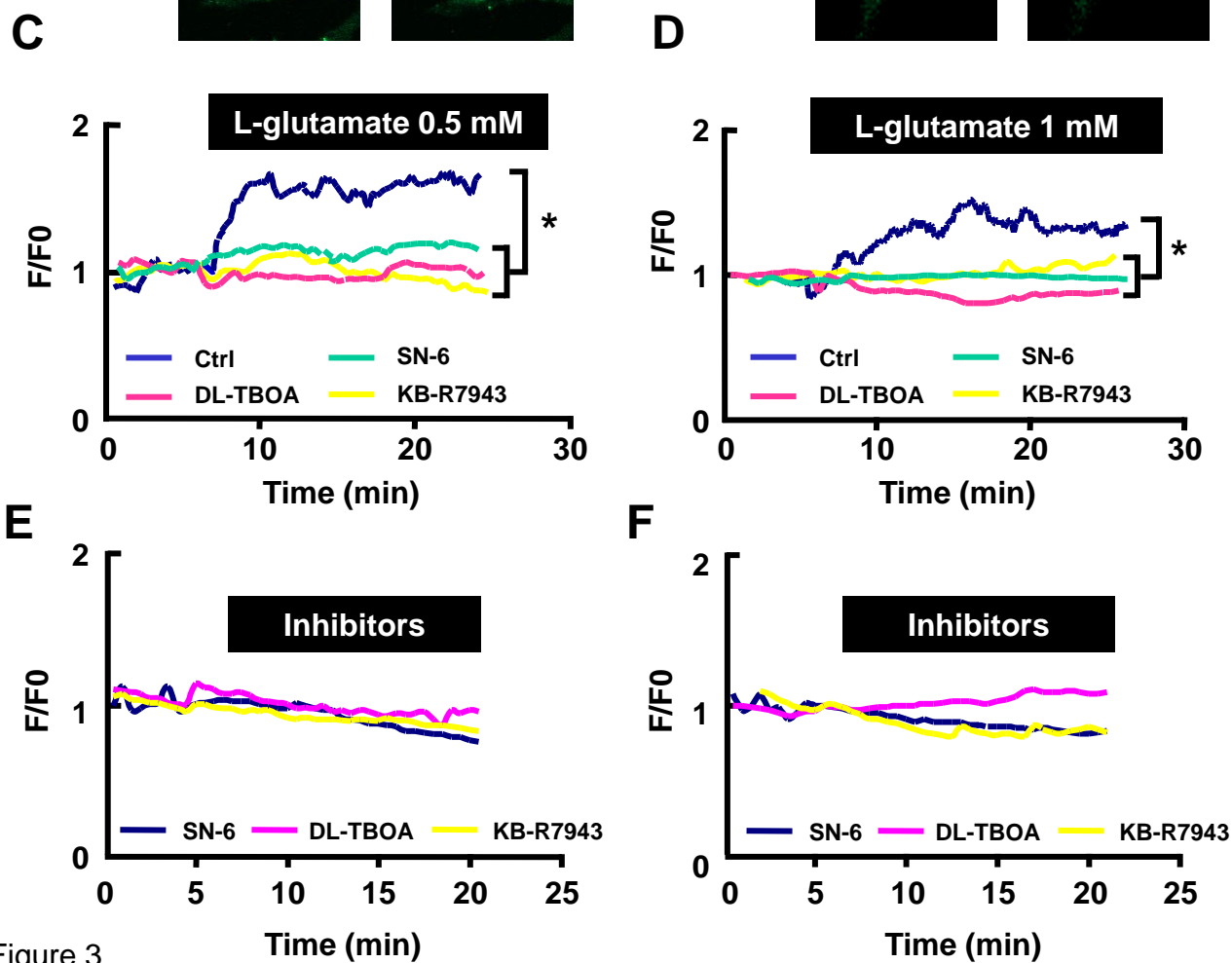
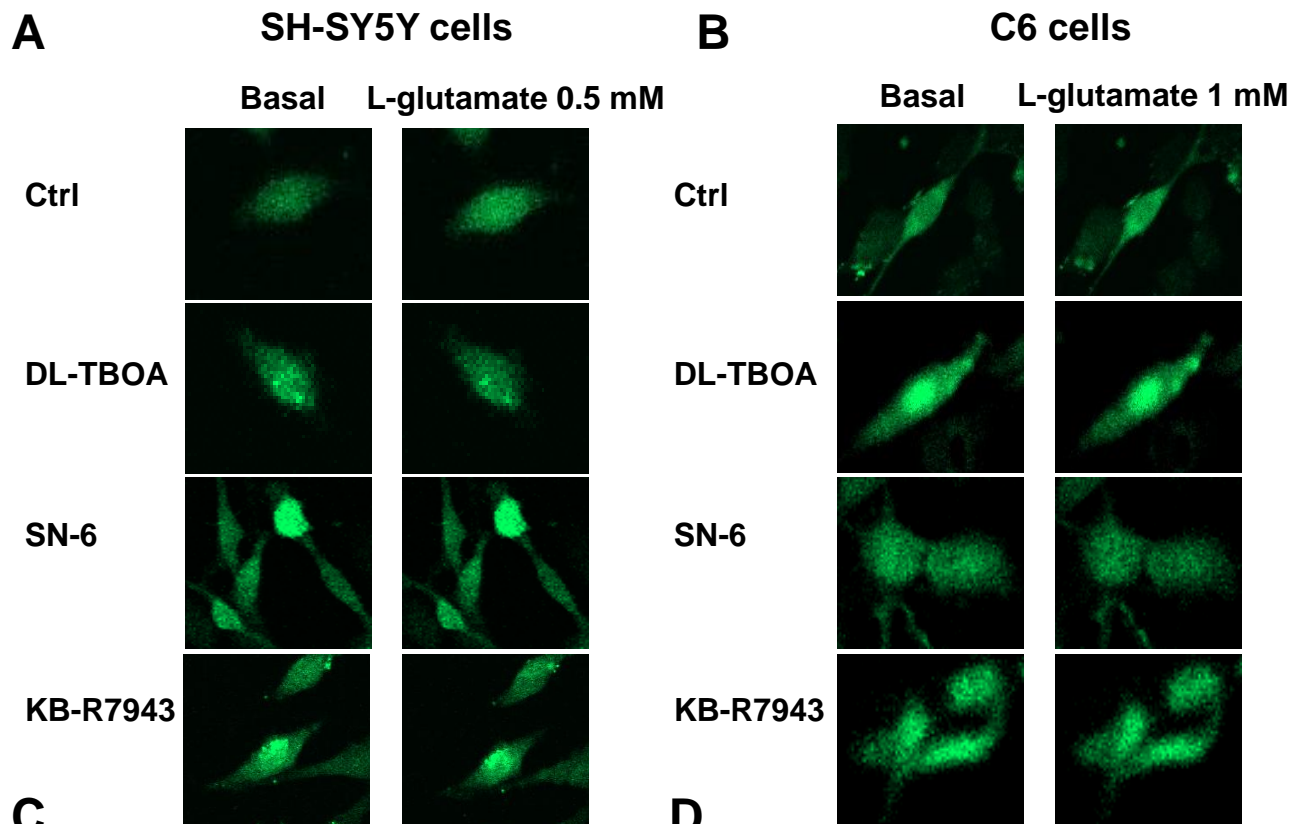


Figure 3

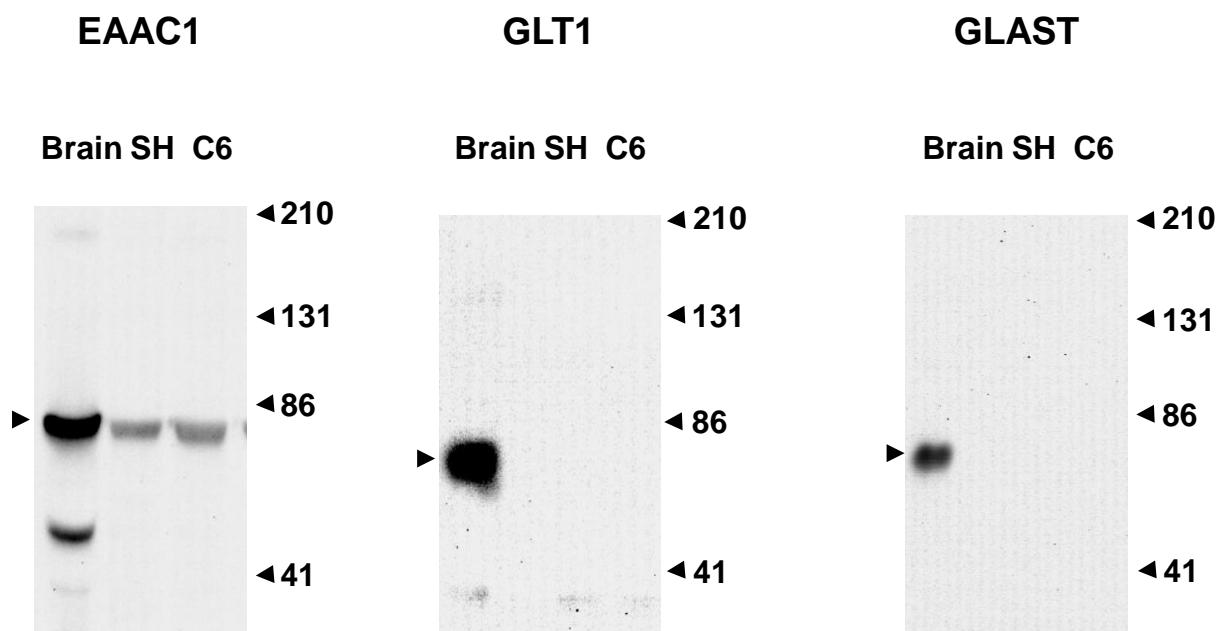
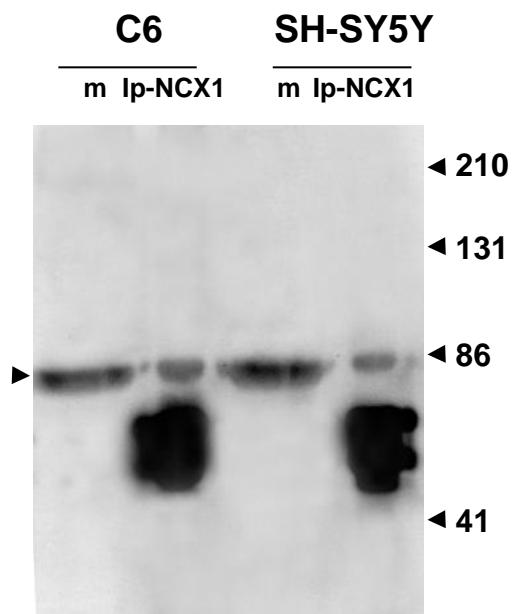
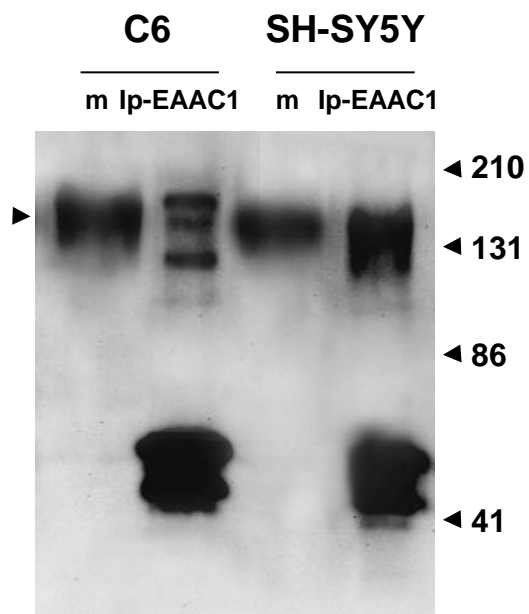
A**B****EAAC1****C****NCX1**

Figure 4

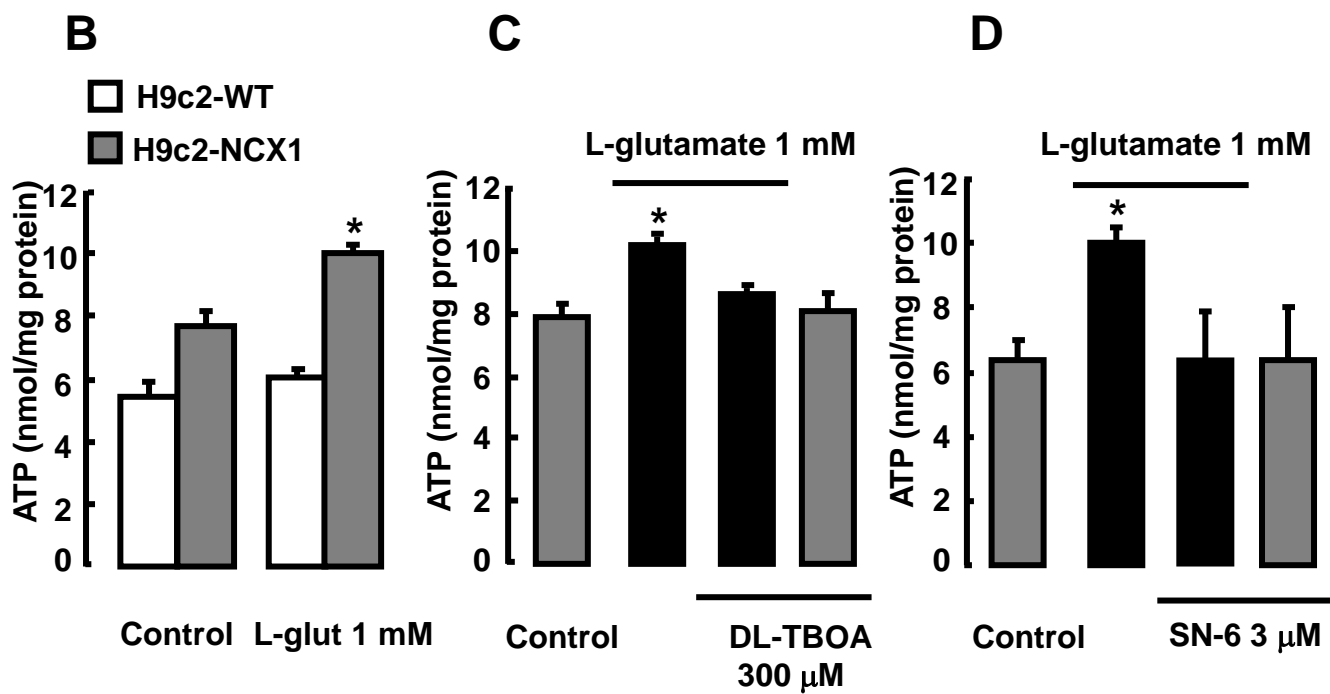
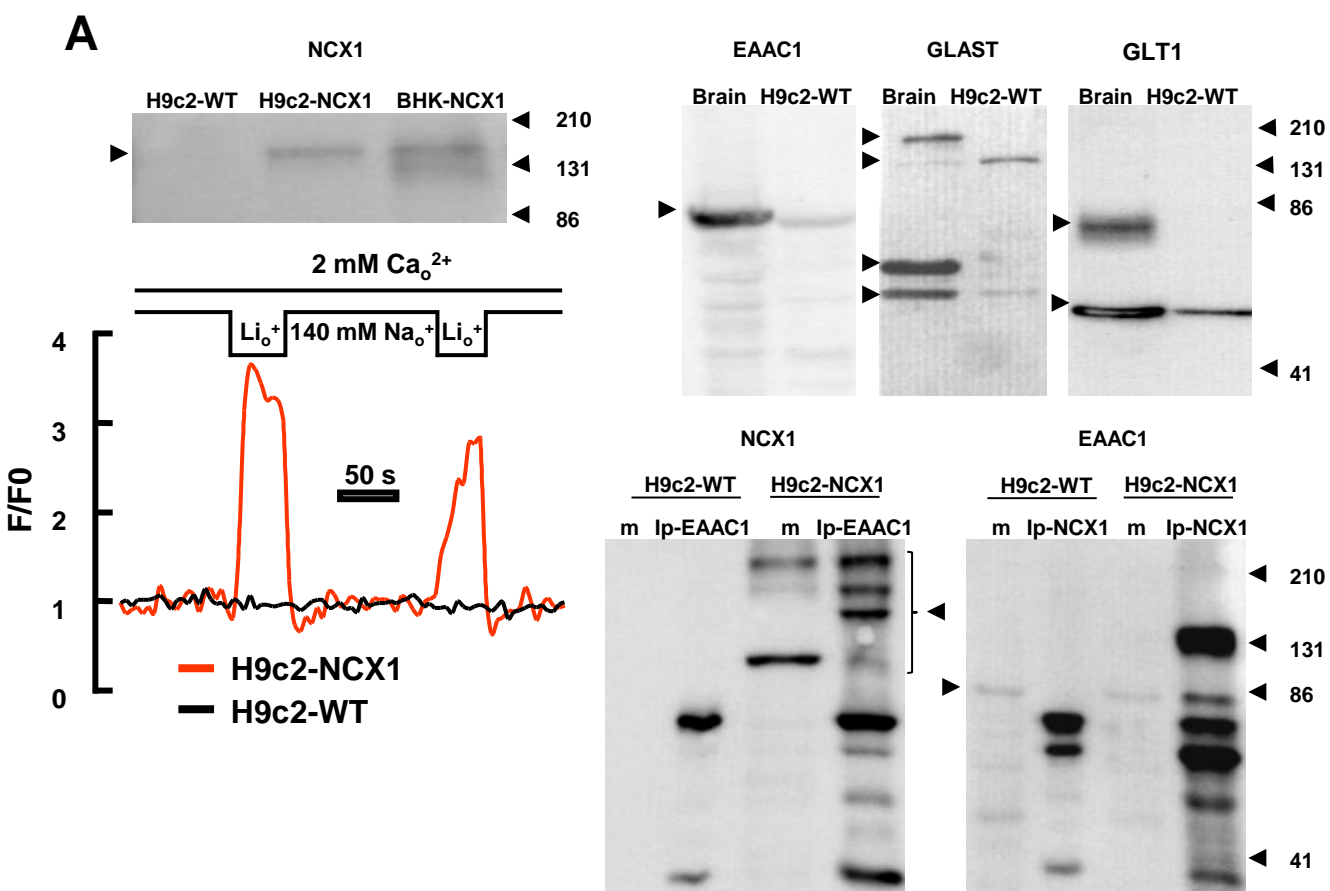


Figure 5

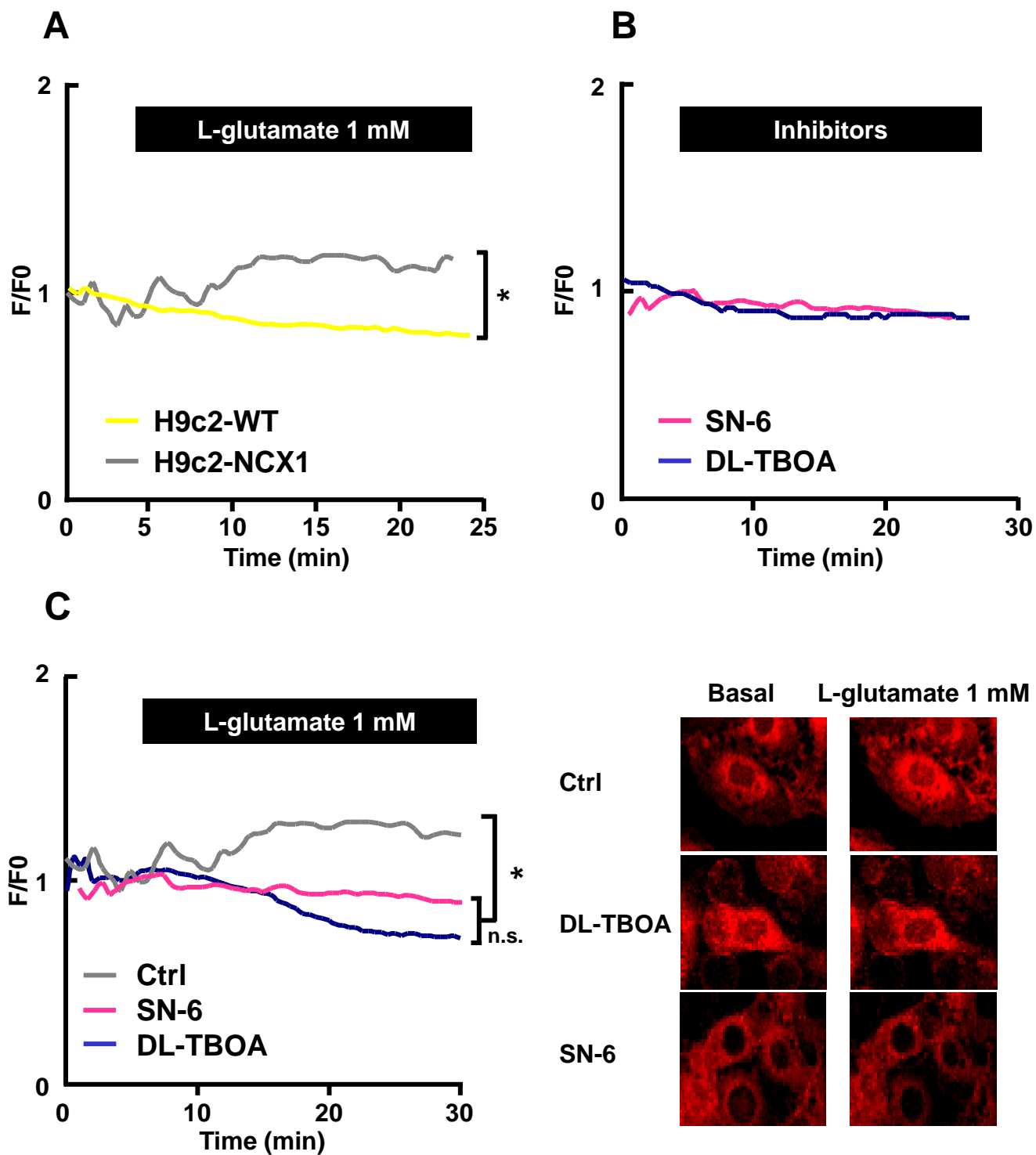


Figure 6

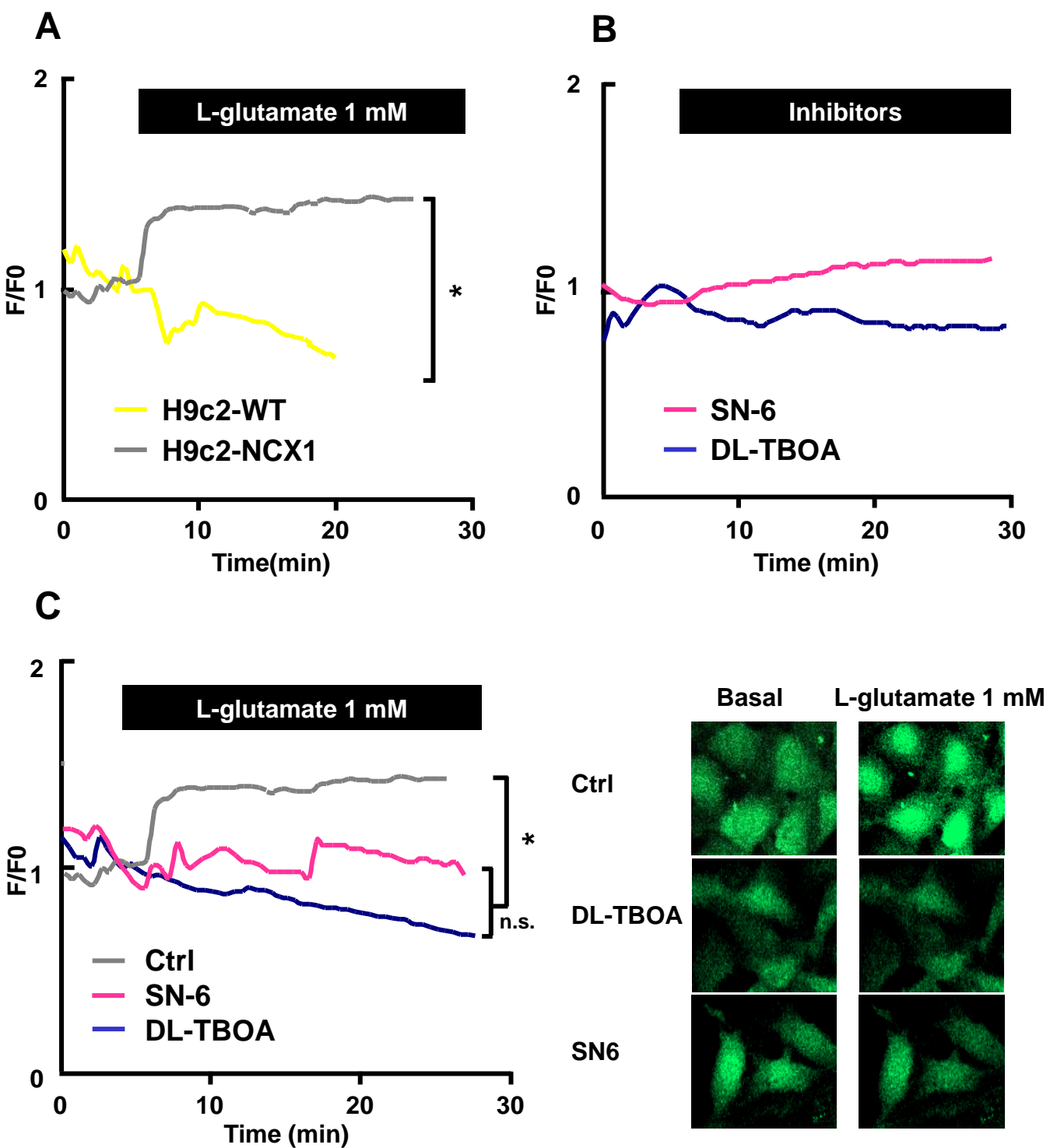


Figure 7

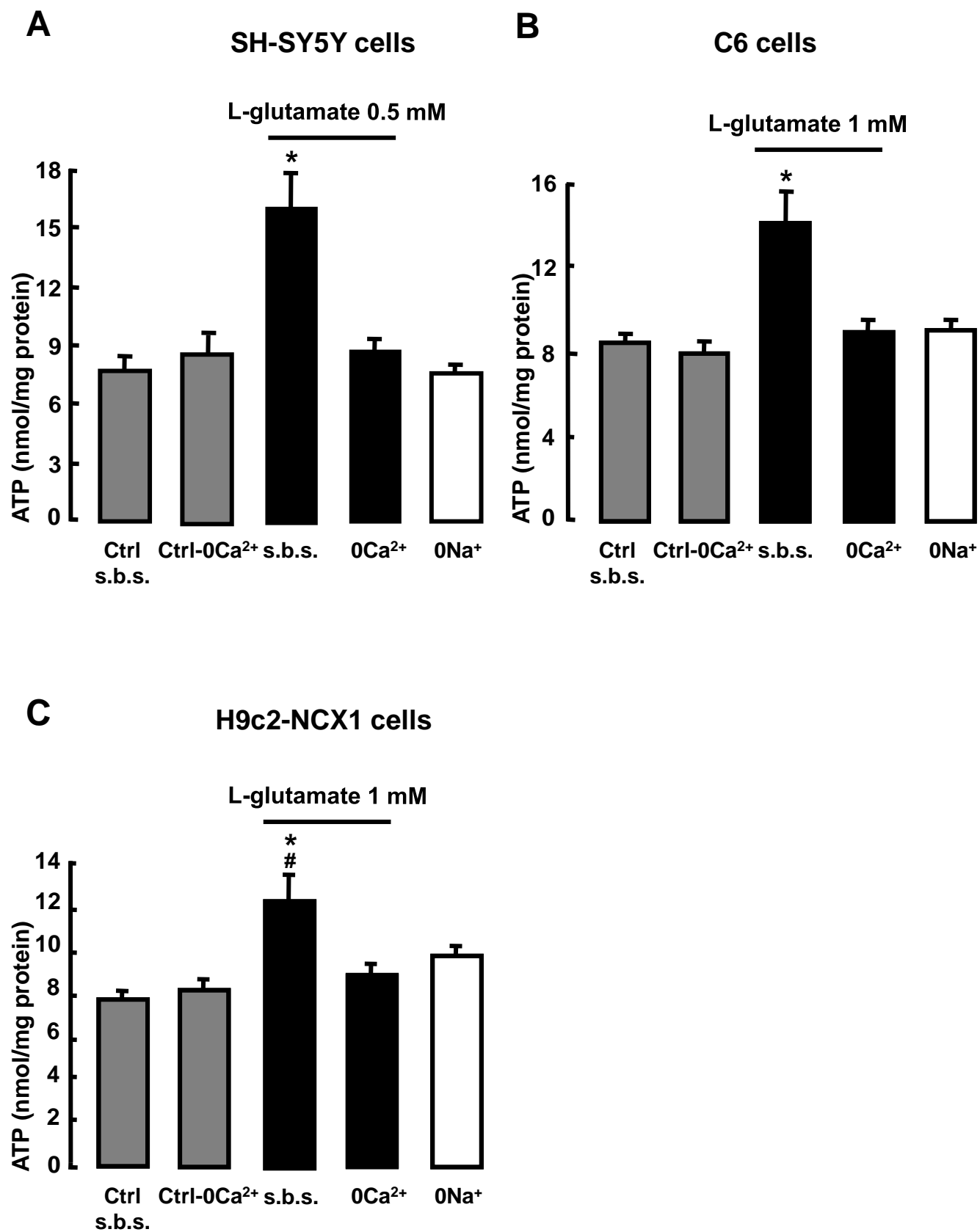


Figure 8